Dispersion and Solubilization of Single-Walled Carbon Nanotubes with a Hyperbranched Polymer

Alexander Star and J. Fraser Stoddart*

Department of Chemistry and Biochemistry, University of California, Los Angeles, 405 Hilgard Avenue, Los Angeles, California 90095-1569

Received March 18, 2002
Revised Manuscript Received June 11, 2002

Introduction

Since their discovery[1] in 1993, carbon single-walled nanotubes (SWNTs) have attracted a lot of attention because of their unique physical, chemical, and mechanical properties.[2] Carbon SWNTs are expected to find applications in numerous technological contexts,[2] e.g., as ultrahigh strength materials, in field emission displays, as supercapacitors, and in molecular computers. There is, however, a fundamental impediment to these developments. The strong van der Waals attractions that exist[3] between the surfaces of the SWNTs lead to rope formation by the single tubes, and render carbon nanotubes highly insoluble and difficult to process for many potential applications. For instance, to enhance the role of nanotubes as reinforcing rods in high-strength composites, the large aggregates of nanotubes invariably present in samples need to be broken up and dispersed in the polymer matrixes. Then, in a nanotechnological context, single nanotubes are much preferred over bundles, not just for reasons of size but also because ropes are much less flexible than SWNTs and hence more difficult to align using flow techniques.[4] And then again, the conductivity of carbon nanotubes depends[5a] strongly on their degree of aggregation. For example, although the so-called armchair nanotubes, which are predicted to be metallic,[5b,c] do indeed behave[5a] like metals when they are isolated from each other, when they are grouped together in bundles, these particular nanotubes act[5a] more like semiconductors.

It is known[6] that certain polymers can wrap themselves around carbon nanotubes and disrupt the van der Waals interactions that cause SWNTs to aggregate into bundles. Nanotube/poly{(*m*-phenylenevinylene)-*co*-[(2,5-dioctoxy-*p*-phenylene)vinylene]} (PmPV)-based composites have received much attention[7,8] recently for, not only providing solubilized nanotubes, but also for the fabrication of light-emitting diodes.[7a] However, most polymers are reasonably flexible and can wrap themselves either around SWNTs or around ropes of nanotubes without exhibiting much discrimination toward their different diameters. Thus, more rigid macromolecules, which can either thread themselves onto or clip themselves around only SWNTs, would be expected to be even more efficient at breaking up nanotube bundles. Ideally, these macromolecules should possess the same kind of PmPV-like structure with its conjugated character that makes it so effective at solubilizing carbon nanotubes. Stilbenoid dendrimers[9] are not only similar to PmPV-based polymers in their properties, but they also possess more spherical shapes and contain pockets of rather well-defined dimensions. Such dendrimers have been prepared up to their third generation by Meier[10] in a multistep convergent synthesis. By contrast, a one-step polymerization using similar building blocks should generate hyperbranched polymers. In this paper, we present the synthesis and characterization of a hyperbranched variant of the PmPV polymer and report on its ability to solubilize SWNTs.

* To whom correspondence should be addressed. Phone: (310) 206-7078. Fax: (310) 206-1843. E-mail: stoddart@chem.ucla.edu.

Results and Discussion

Recently, we have described[8] a helical PmPV-based polymer which can wrap itself around carbon nanotubes, making them soluble in organic solvents without altering their constitutions. The polymer backbone—a conjugated π-extended system—interacts strongly with carbon nanotubes. From extensive atomic force microscopy (AFM) studies and two-photon fluorescence experiments, we discovered[8] that the polymer wraps itself around bundles of carbon nanotubes with the bundle diameter decreasing as the polymer concentration is increased. By molecular modeling, we have established[8] that PmPV is a flexible polymer, which can adjust itself to different bundle diameters such that a size exclusion mechanism is unlikely. On increasing the polymer concentration, more of the carbon nanotube surface becomes covered with the polymer and the bundle size decreases. On the other hand, if one could use macromolecules with well-defined cavities to encircle carbon nanotubes, then it might be possible to isolate single tubes selected according to their diameters. Ideally, these macromolecules should possess the same PmPV unit with that conjugated character which makes it so effective at solubilizing carbon nanotubes. Stilbene dendrimers have a similar π-extended system and possess cavities of defined size. To shed some understanding on the interaction of SWNTs with such a hyperbranched polymer, we decided to perform some molecular modeling. The calculations were simplified by selecting an *all-trans*-stilbene dendrimer without any substituents.[11] We found that, in generations up to 3, the molecules remain planar with no interference from side branches. There are three well-defined pockets, which are accessible from the outside in the third-generation dendrimer. From the fourth generation upward, the molecular planarity is affected by interchain steric hindrance and the dendrimer branches start to bend in a helical fashion so as to close up the pockets. The diameter (based on interatomic distances) of the pockets is about 2 nm, which fits very nicely with the diameter (1.4 nm) of the carbon (10,10)-SWNTs. In the complex (Figure 1) of (10,10)-SWNTs with the third-generation dendrimer, the phenylene rings in the polymer backbone rotate to accommodate the nanotube in the pocket. One can envisage two different mechanisms for the formation of the complex: (1) slippage of the dendrimer onto SWNTs from the end of the nanotube or (2) clipping of the nanotube from the side. Considering the length/diameter ratio (a few micrometers/1.4 nm) of SWNTs and their existence in bundles, slippage mechanism 1 is the less preferred one of the two, although, at higher generations, the periphery of the dendrimer will become crowded and clipping mechanism 2 may be seriously impaired. All three pockets

10.1021/ma0204150 CCC: $22.00
Published on Web 08/08/2002

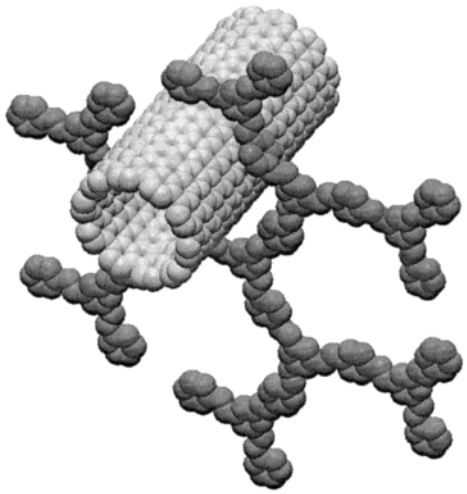

Figure 1. Molecular modeling of the G-3 of an ideal stilbenoid dendrimer (without alkoxy substituents on phenylene rings) and (10,10)-SWNT.

of the dendrimer molecule will be more or less equally available for accommodation by nanotubes. Their occupancy will be a function of the SWNT/polymer ratio.

A multiple Wittig condensation of the bis(triphenylphosphonium) salt **1** and isophthaldehyde (**2**) was used[8] for the preparation (Scheme 1) of poly{(*m*-phenylenevinylene)-*co*-[(2,5-dioctoxy-*p*-phenylene)vinylene]} (PmPV). Alternatively, the same PmPV polymer can be made by the multiple Wittig condensation of 2,5-dioctyloxyterephthaldehyde (**3**) and the bis(triphenylphosphonium) salt **4**. 2,5-Dialkoxyterephthaldehyde is a known[12,13] precursor for the synthesis of conducting polymers. These dialdehydes are usually obtained from 2,5-bis(chloromethyl)-1,4-bis(alkoxy)benzene, either by a three-step synthesis[13b] or by a one-step Sommelet reaction.[13c] Our attempt at using the one-step Sommelet reaction gave a product in only 4% yield, an outcome which is consistent with the literature.[13c] In this study, **3** (Scheme 2) was prepared in three steps, starting from the commercially available diethyl 2,5-dihydroxyterephthalate, which was *O*-alkylated (K_2CO_3/DMF) with octyl chloride at 80 °C, resulting in the isolation of diethyl

Scheme 1. Synthesis of the PmPV Polymer Using the Wittig Reaction[a]

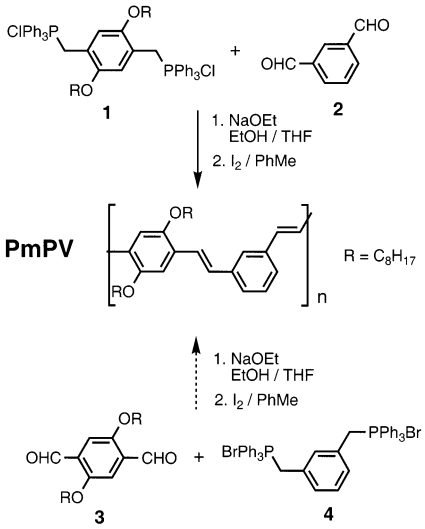

[a] Successful route,[8] solid arrow; unsuccessful approach, dashed arrow.

Scheme 2[a]

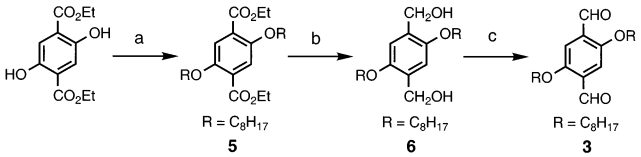

[a] Reagents and conditions: (a) 1-chlorooctane, K_2CO_3, DMF, 80 °C, 41%; (b) $LiAlH_4$, THF, reflux, 96%; (c) PCC, CH_2Cl_2, room temperature, 80%.

2,5-dioctyloxyterephthalate (**5**). This diester was reduced with lithium aluminum hydride in THF, giving 1,4-dioctyloxy-2,5-dimethylhydroxybenzene (**6**), which was then oxidized (PCC/CH_2Cl_2) at room temperature to afford the dialdehyde **3**.

An alternative approach to the synthesis of PmPV, one which involves multiple Wittig reactions between the dialdehyde **3** and 1,3-bis[(triphenylphosphonio)-methyl]benzene dibromide (**4**) did not work. Under typical polymerization conditions, this reaction produced only short oligomers and no PmPV was detected. A possible explanation for this unsuccessful alternative approach to the synthesis of PmPV is the poor solubility of the bis(triphenylphosphonium) salt **4** in the reaction mixture (THF/EtOH), and as a result, an effective excess of the dialdehyde **3** is maintained during the polymerization process.

We decided to take advantage of these results to synthesize a hyperbranched polymer. Usually, hyperbranched polymers are prepared by a one-step self-polymerization of AB_X-type multifunctional monomers.[14] Infinite network formation, which would be observed as gel formation, is not allowed statistically in the case of the self-polymerization of AB_X monomers. If propagation reactions proceed symmetrically and the degree of branching (DB) of the polymer is equal to 1, the architecture of the hyperbranched polymer is eventually the same as that of the corresponding dendron. However, as was suggested in the literature before,[14] the degree of branching of hyperbranched polymers from the one-pot polymerization of AB_2 monomers tends to be close to 0.5. In this work we have used the fact that the core compound 1,3,5-tris[(triphenylphosphonio)methyl]-benzene tribromide (**7**) is not soluble in the reaction mixture (THF/EtOH) and, as a result, there is an effective excess of the dialdehyde **3** present during the polymerization process. Thus, soluble A_2B and AB_2 species formed during the reaction serve as monomers in the polymerization. The core compound **7** reacts with the dialdehyde **3** under the same PmPV polymerization conditions, but with a 1:2 stoichiometry to ensure that the growing hyperbranched polymer will always end with aldehyde functions, thus avoiding gelation. Scheme 3 shows schematically the third-generation dendrimer product (G-3), which has DB = 1, and its possible isomeric hyperbranched polymer (iso-G-3) with DB = 0.5. It should be pointed out that, since hyperbranched polymers at low degrees of branching also possess fractional pockets characteristic of ideal dendrimers, they could be tested for size discrimination in the solubilization of SWNTs.

In common with Wittig reactions of this type, the olefinic double bonds that are produced exist as a mixture of *cis* and *trans* configurations. The proportion of *cis* double bonds in the crude hyperbranched polymer **8′** was about one-third. However, the necessary isomerizations of all the *cis* double bonds to *trans* ones to give

Scheme 3. Synthesis of the Hyperbranched Polymer 8 and Schematic Representations of (a) the G-3 Ideal Dendrimer (DB = 1.0) and (b) Iso-G-3 (DB = 0.5)

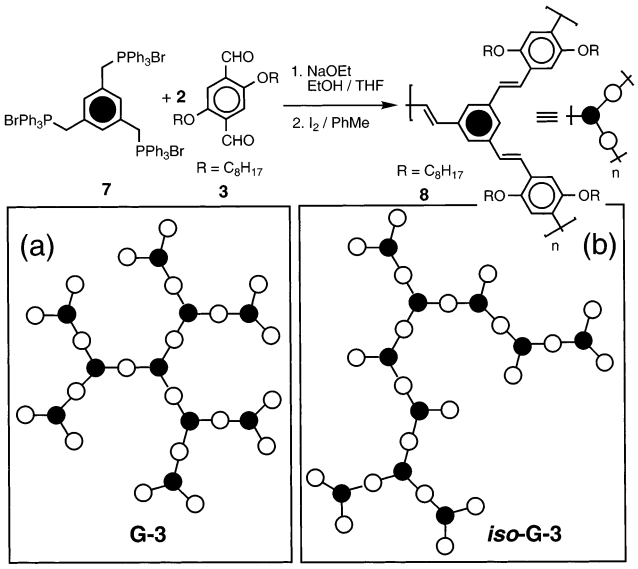

the *all-trans* hyperbranched polymer **8** was achieved by heating the crude polymer in PhMe under reflux in the presence of iodine as a catalyst. Since the resonances, which appear at ca. δ 3.5 and 4.0 in the ^{1}H NMR spectrum of the crude polymer, can be attributed to the protons on the *O*-methylene groups attached to the hydroquinone rings carrying *cis* and *trans* double bonds, respectively, as their nearest neighbors, ^{1}H NMR spectroscopy was employed to follow the course of the isomerization. It was quantitative. ^{1}H NMR spectroscopy also shows the presence of aldehyde end groups to the extent of 50% of an ideal hyperbranched polymer structure, derived from 1:2 stoichiometry of starting materials **7** and **3**. GPC measurements on the hyperbranched polymer **8** show that the number-average molecular weight (M_n) is 15000 and 18000 before and after $CHCl_3$/MeOH precipitation, respectively, corresponding to a generation number for the ideal dendrimer of between 3 and 4. Interestingly, in the polydisperse molecular weight distribution observed by GPC (Figure 2), we can distinguish peaks with molecular weights corresponding to different dendrimer generations. The UV−vis absorption spectrum of the hyperbranched polymer **8** in $CHCl_3$ shows maxima at 336 and

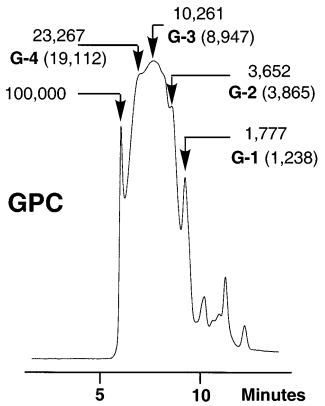

Figure 2. GPC of the hyperbranched polymer **8**. Molecular masses of some peaks were compared to those of different generations of the ideal dendrimer (their mass values presented in parentheses).

403 nm with molar absorption coefficients on the order of 10^4. Compared with PmPV, the absorption bands are all blue shifted (7 nm), an observation which suggests that the incorporation of the extra branching point at the *m*-phenylene group reduces the effective conjugation length and increases the band gap.

We have found that SWNTs can be suspended in solutions of the hyperbranched polymer **8** in $CHCl_3$. An excess of the hyperbranched polymer **8** is necessary to solubilize nanotubes. Sonication in an ultrasonic bath at a 5:1 ratio of the hyperbranched polymer **8** to the SWNTs produced a stable transparent solution. On studying the hyperbranched polymer/SWNT solution by UV/vis spectroscopy, we have found that the hyperbranched polymer bands are broadened in the complex, presumably as a result of $\pi-\pi$ interactions between the SWNTs and the fully conjugated hyperbranched polymer backbone. In common with the PmPV case, the SWNT/hyperbranched polymer complex yields a spectrum with broad absorptions around 650 and 900 nm, corresponding to the band-to-band transitions of pure SWNTs.

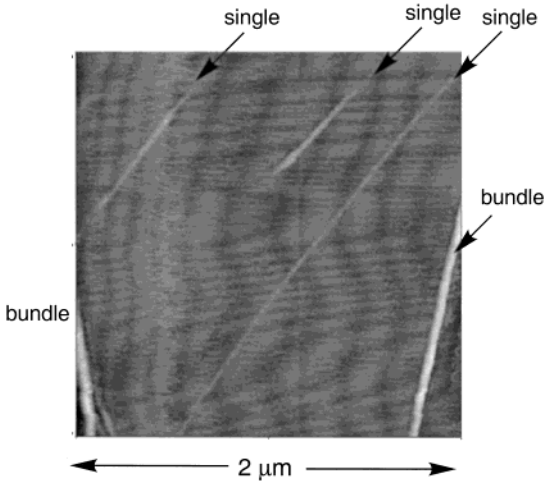

Figure 3. AFM image on a mica wafer of the SWNT/hyperbranched polymer **8** complex, prepared from a solution containing 0.2 mg of SWNTs with 1 mg of **8** in 5 mL of $CHCl_3$.

Noncontact AFM images of the SWNT/hyperbranched polymer samples have indicated a very efficient dispersion of the nanotubes. A typical AFM image which was prepared from a sample that was spin-coated onto a mica wafer is shown in Figure 3. The large number of single tubes[15] and small bundles was detected on analyses of these images. The average diameter of the tubes was calculated, as 1.6 ± 0.5 nm, i.e., twice as small as the average diameter of the nanotubes (3.4 ± 2.4 nm) at the highest PmPV/SWNTs ratio (4:1) in previous studies.[8] The small bundles (typically 2.5 nm) probably correspond to at least three nanotubes inside the pockets of the hyperbranched polymer. The image shows clearly how the single tubes are straight and aligned well with the solvent radial flow which is generated during the spin-coating process.

Conclusions

Compared with polymers, rigid macromolecules, e.g., stilbene dendrimers, possess more two-dimensional shapes and contain pockets of rather well-defined dimensions. Molecular modeling studies of the third-generation stilbenoid dendrimer show that only single

(10,10)-SWNT can fit inside the pockets of the dendrimer, thus providing the possibility of more efficient dispersion of nanotube bundles during their solubilization. In the event, we have synthesized a hyperbranched polymer which exhibits an appropriate degree of branching, and it was found to be more efficient at breaking up nanotube bundles, provided it is employed at higher polymer-to-nanotube ratios than was the "parent" PmPV polymer. Introducing a certain degree of branching into the PmPV polymer makes it more rigid and less efficient when it comes to wrapping bundles of SWNTs, and so more polymeric material is required to achieve a sufficient coverage for nanotube dispersion and solubilizaiton. However, the pockets provided by the hyperbranched polymer offer a better fit for the SWNTs. The outcome is that more single strands of SWNTs are observed on a mica wafer by atomic force microscopy than was the case when the PmPV polymer was used.[8] Our success in employing a synthetic hyperbranched polymer to disperse and solubilize SWNTs in organic solvents is reminiscent of the use of gum arabic[16] and starch[17] to dissolve SWNTs in aqueous solutions.

Experimental Section

Materials and Instrumentation. Chemicals were purchased from Aldrich and used as received. Sodium ethoxide was freshly prepared prior to use from sodium metal and anhydrous ethanol. Solvents were dried, distilled, and stored under argon. **7** was prepared according to a literature procedure.[18] Column chromatography was performed using Merck silica gel 60. Melting points (mp's) were determined on an electrothermal melting point apparatus and are uncorrected. Proton and carbon nuclear magnetic resonance (^{1}H NMR and ^{13}C NMR) spectra were recorded on a Bruker AM360 (^{1}H NMR, 360 MHz; ^{13}C NMR, 90 MHz) spectrometer at 25 °C, using the deuterated solvent as lock and the resudual solvent as internal standard. Electron impact ionization mass spectrometry (EI-MS) was performed on an AUTO-SPEC instrument. Elemental analyses were carried out by Quantitative Technologies Inc. UV−vis spectra were obtained using a Varian Cary 100 Bio spectrophotometer. Absorption measurements of polymeric sample solutions were carried out in chloroform with concentrations of 1.0×10^{-4} and 1×10^{-5} M relative to repeating units in a polymer. Molecular weights of the polymers were determined by using a Dynamax solvent delivery module system, a Styragel HR3 column, and a Dynamax PDA-2 diode array detector, at a flow rate of 1.0 mL/min. All molecular weights were measured against polystyrene standards in tetrahydrofuran.

Diethyl 2,5-Dioctyloxyterephthalate (5). A solution of diethyl 2,5-dihydroxyterephthalate (12.7 g, 50 mmol), 1-chlorooctane (19 mL, 110 mmol), and K_2CO_3 (27.6 g, 200 mmol) in DMF (250 mL) was heated for 7 d at 80 °C. The product was isolated by extraction with Et_2O, washed with H_2O, and dried ($MgSO_4$). Evaporation of the solvent in vacuo gave an oil, which was purified by flash column chromatography (SiO_2, light petroleum/CH_2Cl_2 gradient) to afford the product (6.7 g, 41%), mp 41 °C (MeOH). ^{1}H NMR ($CDCl_3$): δ 7.34 (s, 2H), 4.37 (q, J = 7 Hz, 4H), 4.00 (t, J = 6.5 Hz, 4H), 1.80 (p, J = 6.8 Hz, 4H), 1.47 (p, J = 7 Hz, 4H), 1.39 (t, J = 7 Hz, 6H), 1.37−1.28 (m, 16H), 0.88 (t, J = 6.6 Hz, 6H). ^{13}C NMR ($CDCl_3$): δ 166.1, 151.7, 124.8, 116.6, 69.9, 61.2, 31.8, 29.30, 29.28, 29.22, 26.0, 22.6, 14.2, 14.0. UV−vis ($CHCl_3$, $c = 10^{-4}$ M): λ, nm (ϵ) = 339 (8000). EI-MS: m/z (rel intens) 478.3 (M, 100), 433.3 (M − OEt, 11), 366.2 (M − C_8H_{16}, 13), 254.1 (M − $2C_8H_{16}$, 83), 208.0 (M − $2C_8H_{16}$ − EtOH, 100). $C_{28}H_{46}O_6$ (478.66).

1,4-Dioctyloxy-2,5-dimethylhydroxybenzene (6). A solution of **5** (4.8 g, 10 mmol) in dry THF (30 mL) was added dropwise over 20 min to a suspension of $LiAlH_4$ (1.9 g, 50 mmol) in dry THF (40 mL) at such a rate to maintain a gentle reflux. The reaction mixture was then heated under reflux for an additional 2 h. After the excess of $LiAlH_4$ was quenched with EtOAc and 2 N HCl solution, the product was extracted with CH_2Cl_2 (3 × 120 mL), dried ($MgSO_4$), and evaporated in vacuo to give a white solid (3.8 g, 96%), mp 105 °C ($CHCl_3$). ^{1}H NMR ($CDCl_3$): δ 6.84 (s, 2H), 4.66 (s, 4H), 3.96 (t, J = 6.2 Hz, 4H), 2.37 (br s, 2OH), 1.77 (p, J = 6.8 Hz, 4H), 1.44−1.28 (m, 20H), 0.89 (t, J = 6.8 Hz, 6H). ^{13}C NMR ($CDCl_3$): δ 150.5, 129.0, 112.2, 68.7, 62.1, 31.7, 29.33, 29.26, 29.17, 26.1, 22.6, 14.0. UV−vis ($CHCl_3$, $c = 10^{-4}$ M): λ, nm (ϵ) = 295 (4500). EI-MS: m/z (rel intens) 394.3 (M, 10), 376.3 (M − H_2O, 10), 264.2 (M − C_8H_{16} − H_2O, 10), 152.0 (M − $2C_8H_{16}$ − H_2O, 100). $C_{24}H_{42}O_4$ (394.59).

2,5-Dioctyloxyterephthaldehyde (3). Pyridinium chlorochromate (1.95 g, 9 mmol) was added at room temperature to a clear solution of **6** (1.18 g, 3 mmol) in anhydrous CH_2Cl_2 (50 mL). The color of the solution turned from orange to dark brown. After 2 h, Et_2O (100 mL) was added to the reaction mixture and the precipitate was filtrated through a Celite pad. Evaporation of the filtrate gave a yellow-brown solid, which was recrystallized from Et_2O to afford **3** an analytically pure solid (0.94 g, 80%), mp 75 °C. ^{1}H NMR ($CDCl_3$): δ 10.52 (s, 2H), 7.43 (s, 2H), 4.08 (t, J = 6.5 Hz, 4H), 1.83 (p, J = 6.8 Hz, 4H), 1.47 (p, J = 7 Hz, 4H), 1.36−1.28 (m, 16H), 0.89 (t, J = 7 Hz, 6H). ^{13}C NMR ($CDCl_3$): δ 189.4, 155.2, 129.3, 111.6, 69.2, 31.8, 29.24, 29.17, 29.02, 26.0, 22.6, 14.0. UV−vis ($CHCl_3$, $c = 10^{-4}$): λ, nm (ϵ) = 404 (7400), 275 (18700). EI-MS: m/z (rel intens) 390.3 (M, 42), 278.2 (M − C_8H_{16}, 12), 166.0 (M − $2C_8H_{16}$, 100). Anal. Calcd for $C_{24}H_{38}O_4$ (390.56): C, 73.91; H, 9.81. Found: C, 73.83; H, 9.92.

Crude Hyperbranched Polymer 8′. A 2.5% NaOEt in EtOH solution (0.56 mL, 0.5 mmol) was added dropwise to a solution of **3** (86 mg, 0.22 mmol) and 1,3,5-tris[(triphenylphosphonio)methyl]benzene tribromide (126 mg, 0.11 mmol) in a mixture of anhydrous EtOH (1.5 mL) and THF (2 mL) at ambient temperature. The reaction mixture was stirred for an additional 24 h. The resulting polymer was precipitated twice from MeOH and then dried to afford the crude matherial **8′** (120 mg, 81%) as a yellow resin. ^{1}H NMR ($CDCl_3$): δ 10.46 (s, CHO), 10.32 (s, CHO), 7.60−7.40 (m, 1H), 7.30−6.60 (m, 4H), 4.12−3.83 (m, 4H (*trans* fragment)), 3.60−3.45 (m, 4H (*cis* fragment)), 1.90−1.76 (m, 4H), 1.57 (br, 4H), 1.31−1.23 (m, 16H), 0.90−0.80 (m, 6H).

Hyperbranched Polymer 8. The crude hyperbranched polymer **8′** and I_2 (0.4 mg) were heated under reflux in PhMe (10 mL) for 4 h. The solvent and I_2 were evaporated off under reduced pressure, and the product was dissolved in $CHCl_3$ and precipitated with MeOH. The resulting precipitate was dried to afford the hyperbranched polymer **8** as a yellow resin (90 mg, 61%). ^{1}H NMR ($CDCl_3$): δ 10.47 (s, CHO), 7.64 (s, 1H), 7.64−7.46 (m, 2H), 7.36−7.16 (m, 3H), 4.17−4.00 (m, 4H), 1.98−1.80 (m, 4H), 1.66−1.50 (m, 4H), 1.50−1.10 (m, 16H), 0.90−0.80 (m, 6H). ^{13}C NMR ($CDCl_3$): δ 151.2, 138.0, 128.9, 126.9, 124.1, 111.0, 69.7, 69.3, 69.3, 68.9, 31.8, 29.3, 26.3, 26.2, 22.6, 14.1. UV−vis ($CHCl_3$, $c = 10^{-4}$): λ, nm (ϵ) = 403 (20000), 336 (13800).

Molecular Weight Determinations. The molecular weights and polydispersities (PDIs) of **8** before and after $CHCl_3$/MeOH precipitation (M_w = 30000, PDI = 1.9; M_w = 31000, PDI = 1.7) were determined in THF by using size exclusion chromatography (SEC) and UV detection. The SEC system was calibrated prior to use with polystyrene standards. The GPC measurements of the polymer show that the M_n is 15000 and 18000 (before and after $CHCl_3$/MeOH precipitation, respectively), corresponding to a generation number between 3 and 4. The presence of aldehyde end groups is evident from analyses of NMR spectra.

SWNT/Hyperbranched Polymer Complex. The SWNTs were obtained as a surfactant-stabilized water suspension from Tubes@Rice. The nanotube sheets were typically made by vacuum filtration of ∼1.5 mL of a ∼4 mg mL^{-1} nanotube suspension through a poly(tetrafluoroethylene) filter (Gelman, 25 mm in diameter, 0.2 μm pores). The nanotube sheet (formed over the clear funnel area, which was 15 mm in diameter) was washed with deionized H_2O (5 mL) and then MeOH (5 mL) to remove residual NaOH and surfactant, respectively. These sheets were allowed to dry under vacuum at room temperature

overnight before being peeled from the filter. The typical nanotube sheet weighed ~6 mg. It was then resuspended by sonication (2.5 h) in DMF in a water bath (Branson model 1510, 40 kHz). Then, a DMF aliquot containing 0.2 mg of SWNTs was removed by high vacuum, and a solution of the hyperbranched polymer **8** in $CHCl_3$ was added (1 mg in 5 mL). Sonication for 1 h gave a stable transparent solution.

Atomic Force Microscopy Experiments. After sonication, one drop of the SWNT/PmPV solution was placed on a freshly cleaved 1 cm^2 mica wafer which was subsequently treated with 5 drops of $CHCl_3$ while being spun at 750 rpm to wash off excess of the polymer. AFM images were collected in noncontact mode.

Acknowledgment. This research was supported by the Office of Naval Research and by the National Science Foundation.

References and Notes

(1) Ijima, S.; Ichihashi, T. *Nature* **1993**, *363*, 603−605.
(2) (a) Ajayan, P. M. *Chem. Rev.* **1999**, *99*, 1787−1799. (b) Ajayan, P. M.; Zhou, O. Z. In *Carbon Nanotubes*; Dresselhaus, M. S., Dresselhaus, G., Avouris, Ph., Eds.; *Top. Appl. Phys.* **2001**, *80*, 391−425.
(3) Thess, A.; Lee, R.; Nikolaev, P.; Dai, H.; Petit, P.; Robert, J.; Xu, C.; Lee, Y. H.; Kim, S. G.; Rinzler, A. G.; Colbert, D. T.; Scuseria, G. E.; Tomanek, D.; Fischer, J. E.; Smalley, R. E. *Science* **1996**, *273*, 483−487.
(4) (a) Huang, Y.; Duan, X.; Wei, Q.; Lieber, C. M. *Science* **2001**, *291*, 630−633. (b) Diehl, M. R.; Yaliraki, S. N.; Beckman, R. A.; Barahona, M.; Heath, J. R. *Angew. Chem., Int. Ed.* **2002**, *41*, 353−356. (c) Chen, J.; Weimer, W. A. *J. Am. Chem. Soc.* **2002**, *124*, 758−759.
(5) (a) Ouyang, M.; Huang, J.-L.; Cheung, C. L.; Lieber, C. M. *Science* **2001**, *292*, 702−705. (b) Hamada, N.; Sawada, S.; Oshiyama, A. *Phys. Rev. Lett.* **1992**, *68*, 1579−1581. (c) Saito, R.; Fujita, M.; Dresselhaus, G.; Dresselhaus, M. S. *Phys. Rev. B* **1992**, *46*, 1804−1811.
(6) (a) Yudasaka, M.; Zhang, M.; Jabs, C.; Ijima, S. *Appl. Phys. A* **2001**, *71*, 449−451. (b) Stephan, C.; Nguyen, T. P.; Lamy de la Chapelle, M.; Lefrant, S.; Journet, C.; Bernier, P. *Synth. Met.* **2000**, *108*, 139−149. (c) Shaffer, M. S. P.; Windle, A. H. *Adv. Mater.* **1999**, *11*, 937−941. (d) Jin, Z.; Sun, X.; Xu, G.; Goh, S. H.; Ji, W. *Chem. Phys. Lett.* **2000**, *318*, 505−510. (e) Vigolo, B.; Penicaud, A.; Coulon, C.; Sauder, C.; Pailler, R.; Journet, C.; Bernier, P.; Poulin, P. *Science* **2000**, *260*, 1331−1334.
(7) (a) Curran, S. A.; Ajayan, P. M.; Blau, W. J.; Carroll, D. L.; Coleman, J. N.; Dalton, A. B.; Davey, A. P.; Drury, A.; McCarthy, B.; Maier, S.; Strevens, A. *Adv. Mater.* **1998**, *10*, 1091−1093. (b) Curran, S. A.; Davey, A. P.; Coleman, J. N.; Dalton, A. B.; McCarthy, B.; Maier, S.; Drury, A.; Gary, D.; Brennan, M.; Ryder, K.; Lamy de la Chapelle, M.; Journet, C.; Bernier, P.; Byrne, H. J.; Carroll, D.; Ajayan, P. M.; Lefrant, S.; Blau, W. *Synth. Met.* **1999**, *103*, 2559−2562. (c) Coleman, J. N.; Dalton, A. B.; Curran, S.; Rubio, A.; Barklie, R. C.; Blau, W. J. *Adv. Mater.* **2000**, *12*, 213-216. (d) McCarthy, B.; Coleman, J. N.; Czerw, R.; Dalton, A. B.; Carroll, D. L.; Blau, W. J. *Synth. Met.* **2001**, *121*, 1225−1226. (e) in het Panhuis, M.; Munn, R. W.; Blau, W. J. *Synth. Met.* **2001**, *121*, 1187−1188.
(8) Star, A.; Stoddart, J. F.; Steuerman, D.; Diehl, M.; Boukai, A.; Wong, E. W.; Yang, X.; Chung, S.-W.; Choi, H.; Heath J. R. *Angew. Chem., Int. Ed.* **2001**, *40*, 1721−1725.
(9) (a) Díez-Barra, E.; García-Martínez, J. C.; Merino, S.; Rey, R.; Rodríguez-López, J.; Sánchez-Verdú, P.; Tejeda, J. *J. Org. Chem.* **2001**, *66*, 5664−5670 and references therein. (b) Meier, H.; Lehmann, M.; Kolb, U. *Chem.—Eur. J.* **2000**, *6*, 2462−2469. (b) H. Meier and M. Lehmann, *Angew. Chem., Int. Ed.* **1998**, *37*, 643−645.
(10) Lehmann, M.; Schartel, B.; Hennecke, M.; Meier, H. *Tetrahedron* **1999**, *55*, 13377−13394.
(11) Molecular modeling of both the stilbene dendrimer and the dendrimer complex with short (10,10)-SWNTs was carried out as follows. After construction of the relevant structures within the INPUT submode of MacroModel 5.5, the system was minimized using the AMBER force field. The structure was then allowed to equilibrate over the course of a 100 ps (1.5 fs time steps) molecular dynamics simulation at 300 K, before being minimized once more to provide superstructures such as that displayed in Figure 1.
(12) (a) Barashkov, N. N.; Olivos, H. J.; Ferraris, J. P. *Synth. Met.* **1997**, *90*, 41−47. (b) Chen, S.-A.; Chang, E.-C. *Macromolecules* **1998**, *31*, 4899−4907.
(13) (a) Greenham, N. C.; Moratti, S. C.; Bradley, D. D. C.; Friend, R. H.; Holmes, A. B. *Nature* **1993**, *365*, 628−630. (b) Moratti, S. C.; Cervini, R.; Holmes, A. B.; Baigent, D. R.; Friend, R. H. *Synth. Met.* **1995**, *71*, 2117−2120. (c) Liu, Y.; Yu, G.; Li, Q.; Zhu, D. *Synth. Met.* **2001**, *122*, 401−408.
(14) (a) Jikei, M.; Kakimoto, M. *Prog. Polym. Sci.* **2001**, *26*, 1233−1285. (b) Lin, T.; He, Q.; Bai, F.; Dai, L. *Thin Solid Films* **2000**, *363*, 122−125.
(15) AFM cannot, however, distinguish between individual nanotubes lying side by side to form a continuous bundle where all nanotubes are in contact with the surface. AFM resolution in the *xy* plane is orders of magnitude worse than that in the *z* direction. So we assume that the nanotube diameters correspond to the measured heights in the AFM scans of nanotubes on a mica surface.
(16) Bandyopadhyaya, R.; Nativ-Roth, E.; Regev, O.; Yerushalmi-Rozen, R. *Nano Lett.* **2002**, *2*, 25−28.
(17) Star, A.; Steuerman, D. W.; Heath, J. R.; Stoddart, J. F. Starched Carbon Nanotubes. *Angew. Chem., Int. Ed.* **2002**, *41*, 2508−2512.
(18) Stork, W.; Mannecke, G. *Makromol. Chem.* **1975**, *176*, 97.

MA0204150